รายงานการวิจัย

จอยท์ ทรานฟอร์ม คอรีเลเตอร์ โดยใช้ภาพอ้างอิงแบบบีบอัดสำหรับการ
ทดสอบแบบไม่ทำลาย

Joint Transform Correlator by Using Compressed Reference Images for
Non-destructive Testing

ผู้วิจัย

หัวหน้าโครงการ
Assoc. Prof. Dr. Joewono Widjaja
สาขาวิชาเทคโนโลยีเลเซอร์และโฟตอนนิกส์
สำนักวิชาวิทยาศาสตร์

มีนาคม 2550

Acknowledgement

บทคัดย่อ

เพื่อเป็นการแก้ปัญหาเรื่องพื้นที่จัดเก็บ และปรับปรุงการตอบสนองทางเวลาของระบบทดสอบแบบไม่ทำลาย จึงได้ทำการศึกษาทั้งในเชิงทฤษฎีและปฏิบัติ ในการสร้างจอยท์ทรานฟอร์มคอร์รีเลเตอร์แบบเวลาจริงโดยใช้ภาพอ้างอิงบีบอัด ภาพที่ใช้ในการทดสอบคือภาพสองภาพที่มีความเปรียบต่างและความถี่เชิงตำแหน่งต่างกัน ผลลัพธ์ที่ได้ช่วยยืนยันความสามารถนำไปใช้งานจริงได้ของระบบคอร์รีเลเตอร์ซึ่งใช้ภาพอ้างอิงแบบบีบอัด อย่างไรก็ตามผลของสัญญาณรบกวนแอดดิทีฟต่อประสิทธิภาพการตรวจสอบของระบบที่ได้นำเสนอนั้น มีมากกว่าผลที่เกิดจากการบีบอัด สิ่งนี้อาจเกิดขึ้นจากสัญญาณรบกวนสเป็คเคิล ซึ่งเกิดขึ้นตามธรรมชาติจากการใช้ระบบเชิงแสงแบบโคฮีเรนท์

Abstract

In order to solve storage problem and improve time response of non-destructive testing systems, real-time implementation of joint transform correlator by using compressed reference images are theoretically and experimentally studied. Two images with different spatial-frequency contents and contrast are used as test scenes. The results confirm feasibility of implementing the correlator system with compressed reference images. However, the effect of noise on the detection performance of the proposed system is more severe than that of the compression. This may be caused by an additional speckle noise which is inherently generated as a result of coherent nature of the optical system.

Contents

List of Figures

List of Tables

Chapter 1

Introduction

1.1 Background and Significance

In the field of optical metrology, laser light has been widely used as a tool for non-destructive testing. By illuminating objects or specimens being studied, its diffracted or scattered light is detected and then analyzed in order to extract the desired information. One of useful methods for performing non-destructive testing is an in-line holography [1-5]. In our previous work, a new method for extracting automatically size of small object and its position from in-line holograms by using joint transform correlator (JTC) has been proposed [6]. In the proposed method, the in-line hologram illuminated by a collimated laser beam is placed on three-axis motorized stage controlled by a computer where a set of reference objects has been stored. The reconstructed image of the target object originated from a certain 3-D location is captured by a CCD sensor. The captured image of the target and the reference image stored in a computer system are displayed side-by-side on an electrically-addressed spatial light modulator (EASLM). The joint transform correlation of the target and the reference images is then optically computed. When the size and shape of the target matches to the reference, the JTC gives sharp correlation peak. Thus, the size and position of the target object can be determined.

Although this method is indeed useful for analyzing irregularly shaped particles or images, it suffers from several limitations such as: first, the process of displaying the target and the reference images onto the EASLM introduces a time delay that is caused by a serial nature of signal communication between the computer and the EASLM. This time delay is dependent upon the file size of the images. Second, the analyzing system requires a huge number of reference particles to be stored as database in the computer. Thus, the application of the JTC to non-destructive holographic testing requires considerable storage capability.

One practical approach to solve these problems is to compress the reference images. By applying digital image compression such as that developed by the Joint Photographic Experts Group (JPEG) [7], the time delay occurred during a process of transferring the image from the computer to the EASLM could be reduced and less storage will be required for storing the database. Therefore, an implementation of the real-time JTC by using the compressed reference images has advantages in that it reduces stringent requirement of the storage and speeds up the recognition time. However, in image compressions, the number of bits needed

to represent an image is reduced by discarding spatial and spectral redundancies. As a consequence, the loss of information contents of the reference image may degrade the correlation performance of the JTC. Therefore, the experimental study of the effects of image compression on the JTC is indeed important.

1.2 Objectives

1. To study experimentally performance of the JTC with compressed reference images for non-destructive testing

2. To study effect of noise presence in the target and contrast difference between the target and the reference images

1.3 Scope

Two images with different spatial-frequency contents and contrast are employed as a target and a reference images. In practice, use of CCD image sensors for capturing input targets from outside world gives non ideal images. Thus, this work takes into account a presence of noise in the input and a contrast difference between the target and the reference that may rise due to unbalance illuminations. Single- and multiple-target detections are done by means of computer simulations and experiments. The reference images are compressed into the JPEG file format by using ACDSee software (ACD Systems Ltd.) with different quality factor (QF) whose value is varied from 100 to 0. High value of the QF discards less information than that of the small value. Thus, the higher the value of the QF, the better the image quality and the bigger the file size of the compressed image.

1.4 Expected Benefit

The result obtained from this research project can solve storage problem and improve time response of non-destructive testing by using joint transform correlator with compressed reference images.

Chapter 2

Joint Transform Correlation

The JTC was first proposed by Weaver and Goodman in the 1960's [8]. In the JTC, two spatial patterns to be correlated are placed side-by-side in the front focal plane of a Fourier transforming lens. By illuminating these patterns with a collimated coherent light, a joint Fourier spectrum is produced in the back focal plane of the lens. The produced joint Fourier spectrum of the two patterns is then recorded on a photosensitive medium, such as photographic film, installed at this plane. Finally, the recorded power spectra are optically re-Fourier transformed to produce the output correlation. The correlation consists of three terms: the dc term, and two symmetric cross-correlation of the two patterns. The locations of the symmetric terms are related to the locations of the target and the reference patterns in the input plane.
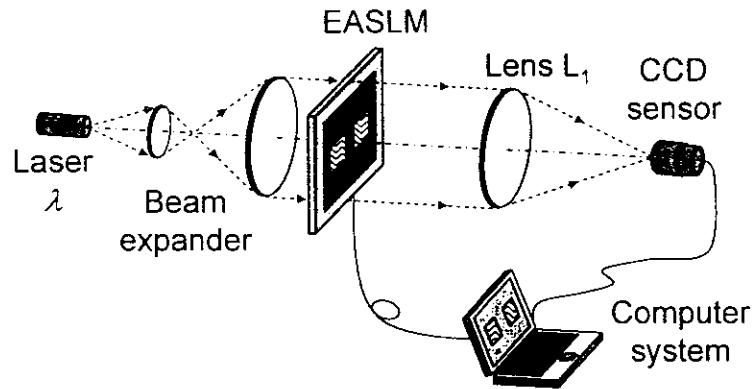
Figure 2.1 A schematic diagram of an optical setup for performing experimental verifications of the JTC with compressed reference images.

Figure 2.1 shows an optical setup for implementing the real-time JTC with the compressed reference images. In our proposed JTC, the input target $t(x,y)$ and the compressed reference $r_c(x, y)$ images are displayed side-by-side onto the EASLM. They can be mathematically written as

$$f(x,y) = r_c(x - x_0, y) + t(x + x_0, y),$$ (1)

where x_0 corresponds to the position of the images in the x direction. Under a presence of an additive white Gaussian noise $n(x, y)$ at the input target and a contrast difference between the target and the compressed reference images, the joint input image can be rewritten as

$$f(x,y) = r_C(x - x_0, y) + c_T t(x + x_0, y) + n(x + x_0, y), \tag{2}$$

where c_T is the amplitude ratio of the target to the reference images. The factor c_T becomes greater, equal, or smaller than 1 when the contrast of the reference image is lower, equal, or higher than that of the target, respectively. After a Fourier transformation by the lens L_1, the JPS captured by the CCD sensor is found to be

$$\begin{aligned}
U(u,v) &= |R_C(u,v)|^2 + c_T^2 |T(u,v)|^2 + |N(u,v)|^2 \\
&\quad + c_T T^*(u,v)N(u,v) + c_T T(u,v)N^*(u,v) \\
&\quad + c_T [R_C(u,v)T^*(u,v)\exp(-j2ux_0) + T(u,v)R_C^*(u,v)\exp(j2ux_0)] \\
&\quad + R_C(u,v)N^*(u,v)\exp(-j2ux_0) + N(u,v)R_C^*(u,v)\exp(j2ux_0), \tag{3}
\end{aligned}$$

where (u,v) are the coordinates at the Fourier plane. $R_C(u,v)$, $T(u,v)$ and $N(u,v)$ are the Fourier transforms of the compressed reference, the target, and the noise, respectively. By displaying the captured JPS onto the EASLM, the second Fourier transformation produces the correlation output at the back focal plane of the lens L_1. The correlation signals corresponding to the sixth, seventh and eighth terms of Eq. (3) can be expressed as

$$I(x,y) = c_T[r_C(x,y) * t(x,y) * \delta(x \pm 2x_0)] + r_C(x,y) * n(x,y) * \delta(x \pm 2x_0), \tag{4}$$

where $*$ denotes correlation. The first term of Eq. (4) corresponds to the desired correlation of the input target with the compressed reference which is scaled by the contrast difference, while the second one is the unwanted correlation of the compressed reference with the noise. Since both terms appear at the same position of $\pm 2x_0$, Eq. (4) indicates that besides the image quality of the compressed reference $r_C(x,y)$, the correlation output depends on both the contrast and the noise. Therefore, it is important to measure the effects of image compression on the correlation performance of the JTC.

4

Chapter 3

Materials and Methods

3.1 Image Compression

(a)

(b)

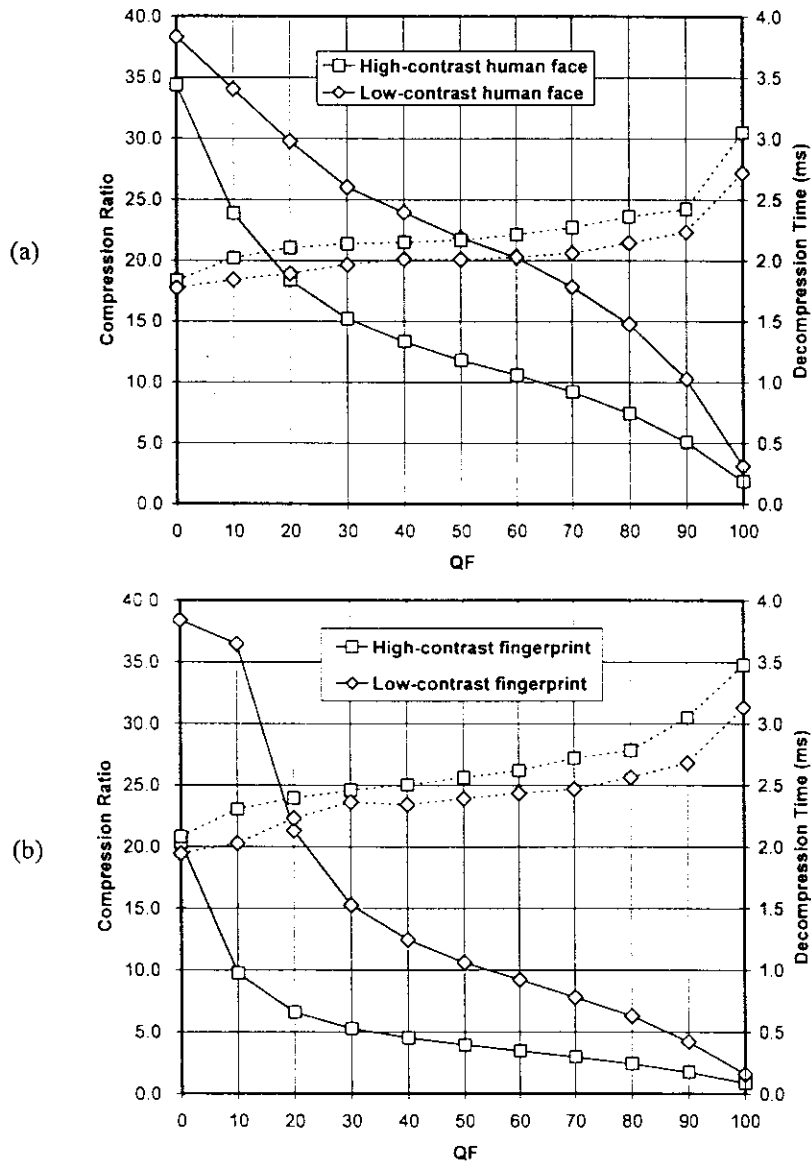**Figure 3.1** Compression ratio and decompression time of the JPEG compressed
(a) human face and (b) fingerprint images as a function of the QF.

Human face and fingerprint images were used as the test scenes with low and high spatial-frequency content. The size of each image was 23 Kbytes and consisted of 124×186 pixels with gray scale levels. Figures 3.1 (a) and (b) show the compression ratios of the human face

and the fingerprint images and their decompression times as a function of the QF. The compression ratio is defined as the ratio of the uncompressed to the compressed file sizes and the decompression time are represented by the solid and the broken lines, respectively. High compression ratio corresponds to a small size of the compressed image. It is clear from the figure that the compression ratio of the human face and the low-contrast images are higher than that of the fingerprint and high-contrast images, respectively. This is due to fact that either the human face or the low-contrast image contains less high spatial-frequency components compared to the fingerprint or the high-contrast image, respectively. Since the JPEG compression is achieved by discarding high spatial-frequency components of digital images, both the human face and the low-contrast images suffer more loss.

The decompression time is a total time required to load the compressed reference images from a hard disk into memory and to decompress them. The time measurements were done by a routine written in Delphi 7. The routine employed a counter utility function of Jedi Code Library [8] as a time counter, while the ImageEn Library was used for image decompression [9]. The time measurements were preformed on Windows-based personal computer with a CPU AMD Athlon 1.8 GHz. By taking the compression ratios into account, it is understood that the decompression time of the compressed high-contrast fingerprint becomes longer than that of the low-contrast one. As the compression ratio becomes smaller, the decompression time reduces. By compression, the decompression time can be minimized by approximately 1.5 times. The figure verifies the usefulness of the compression for improving time response of the real-time JTC systems.

3.2 Computer Simulations and Experimental Verifications

A computer simulation was conducted by computing the joint transform correlation of the target and the compressed reference images with Matlab 5.0 mathematical software. The Fourier spectrum of joint input images consisting of the target and the compressed reference images was first calculated. The power of the resultant Fourier spectra was then computed. The result was inversely Fourier transformed in order to produce the correlation function.

By measuring a ratio of a correlation peak-to-standard correlation deviation of the correlation function and the primary-to-secondary peaks ratio for each corresponding compression quality, the performance of the JTC was quantitatively studied.

In an experimental study, an optical setup shown in Fig. 2.1 was employed to compute the correlation. The target and the compressed reference patterns were displayed side-by-side on a Jenoptik SLM-M/460 electrically-addressed spatial light modulator (EASLM) placed in the

front focal plane of the Fourier transforming lens. Its resolution was 832 × 624 pixels with the pixel size of 27 × 23 µm and the pixel pitch of 32 × 32 µm. The collimated coherent light generated from a HeNe laser operating at wavelength of 632.8 nm was used to illuminate the EASLM. The generated joint Fourier spectra was then recorded by an eight-bit Pulnix TM-2016-8 CCD sensor having a pixel resolution of 1920 × 1080, pixel size and pitch of 7.4 × 7.4 µm. By redisplaying the recorded Fourier spectra onto the EASLM, the correlation output was finally produced at the back focal plane of the lens.

Chapter 4

Results and Discussion

4.1 Computer Simulation Results

Compressed Reference Image	Condition of Single-Target Images			
	Noise Free		Noisy	
	High contrast	Low contrast	High contrast	Low contrast
High-Contrast Fingerprint	Gradual	Gradual	Sudden and significant	Severe
Low-Contrast Fingerprint	Sudden	Sudden	Sudden and significant	Severe
High-Contrast Human Face	No	No	No	No
Low-Contrast Human Face	Very small	Very small	Very small	Very small

Table 4.1 Performance degradation of the single-target detections

by using the JTC with compressed reference images.

Computer simulations were first performed to study the effect of reference compression on the single- and the multiple-target detections [10,11]. Human face and fingerprint images with different contrast were prepared and duplicated into the target and the reference images. In the case of the multiple-target detection, the input scene contained two different images with one of them was identical to the original reference image. From the four types of reference images, the compressed low-contrast human face and the high-contrast fingerprint have the highest and the lowest compression ratios, respectively. The compression ratio of the high-contrast human face is slightly higher than that of the low-contrast fingerprint for the low QF.

The simulation results of the single-target detections show that the effects of compression of the high-contrast human face reference on the detection performance is not significant for all given target scenes. Although the detection performance of the JTC by using the compressed low-contrast human face decreases at the low QF, the degradation due to the noise presence and the contrast difference is small. Besides being sensitive to noise, the

8

correlation performance of this correlator depends on the compression, where the degradation for the low-contrast fingerprint is more significant in comparison with the high contrast. The performance degradation of the correlator used for single-target detection is summarized in Table 4.1.

Compressed Reference Image	Condition of Multiple-Target Images			
	Noise Free		Noisy	
	High contrast	Low contrast	High Contrast	Low contrast
High-Contrast Fingerprint	Gradual	Gradual and significant	Gradual and significant	Severe
Low-Contrast Fingerprint	Sudden	Sudden and significant	Sudden and significant	Severe
High-Contrast Human Face	No	No	No	No
Low-Contrast Human Face	Very small	Very small	Very small	Very small

Table 4.2 Performance degradation of the multiple-target detections by using the JTC with compressed reference images.

The performance degradation of the multiple-target detection using the JTC with compressed reference images is summarized in Table 4.2. When the reference image has low spatial-frequency contents such as the human face image, the effects of compression of the reference on the multiple-target detection by using this correlator is not significant for all given target scenes regardless of the noise and the contrast difference. This is an agreement with the previous study of the single-target detection. Our study shows that in contrast with the use of the compressed reference with low spatial-frequency contents, the multiple-target recognition by using the compressed reference with high spatial-frequency contents is not only determined by the contrast, but also the noise and the compression as well. Finally, it is worth mentioning that the compression of the low-contrast reference with high spatial-frequency contents may yield false alarms.

4.2 Experimental Results

The experimental verifications of the single- and the multiple-target detection by using the JTC with compressed reference images were accomplished by using the optical setup shown

in Fig. 2.1 [12]. Unlike the simulation works, the low-contrast image was not employed, because limited contrast ratio of the used EASLM prevented efficient display of images with small variation of gray-level pixels.
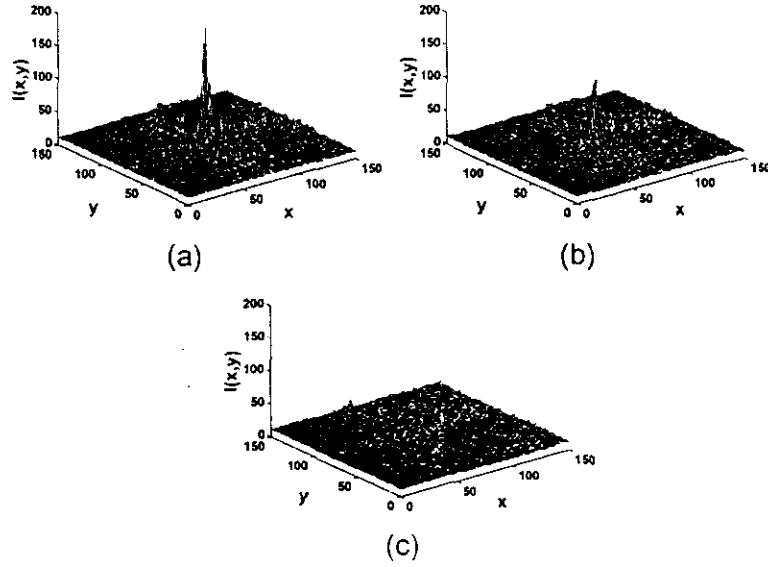
4.2.1 Single-Target Detections

Figure 4.1 Experimental results of the single-fingerprint detection. (a) Autocorrelation output of the uncompressed fingerprint and cross correlation outputs by using the compressed reference (QF = 10) under a situation that the target is: (b) noise free and (c) noisy (σ^2=1).

Figures 4.1(a), (b), and (c) show the experimental results of the fingerprint detections. The autocorrelation peak of the uncompressed fingerprint shown in Fig. 4.1(a) is almost two times higher than the cross correlation peak generated by using the compressed fingerprint with QF = 10 shown in Fig. 4.1(b). This is the effect of the compression that degrades the reference image. Figure 4.1(c) shows the output of the correlation of the noisy fingerprint target with variance σ^2 =1 and the compressed fingerprint reference with QF = 10. It is clear that the correlation peak is degenerated. This is because besides the additive noise, the sinusoidal fringes of the joint power spectra are corrupted by a speckle noise that is inherently generated by light scattering and multiple internal reflections from the EASLM1 and the surface of the sensor. Therefore, the correlation peak cannot be detected.
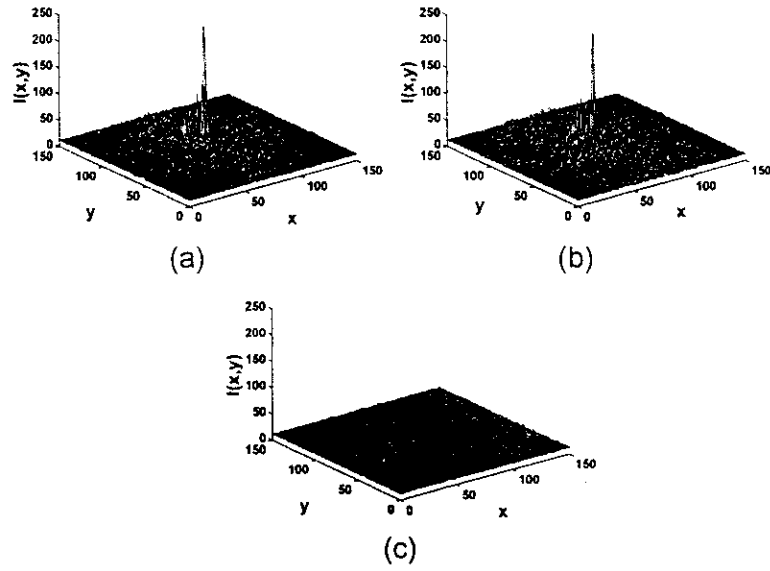
Figure 4.2 Experimental results of the single-human-face detection. (a) Autocorrelation output of the uncompressed human face and cross correlation outputs using the compressed reference (QF = 10) under a situation that the target is: (b) noise free and (c) noisy ($\sigma^2=1$).

The experimental outputs of the single human face detection are shown in Figs. 4.2(a), (b), and (c). When the noise-free human face target is detected by the reference image compressed at QF = 10, the correlation output shown in Fig. 4.2(b) decreases slightly. However, its peak is almost as sharp as the autocorrelation output shown in Fig. 4.2(a). In comparison with the outputs of the fingerprint detections shown in Fig. 4.1, the correlation planes of Figs. 4.2(a) and (b) appear to be noisier. This occurs because in order to capture more fringes in the higher frequency components, the recording of the joint power spectra is done without a use of a ND filter. Consequently, the low-frequency components of the joint power spectra are clipped. As the clipped power spectrum is subsequently displayed onto the EASLM, besides more light is diffracted more speckle noise occurs at the correlation output. Thus, although the peak height is high the speckle noise increases. Moreover, as a blocking artifact [7] caused by the compression increases, more low-frequency components of the power spectra are clipped. This in turn increases further the speckle noise. The correlation output of the noise-corrupted target with the variance $\sigma^2 =1$ is shown in Fig. 4.2(c). For the same reason as before, the correlation peak can not be observed.
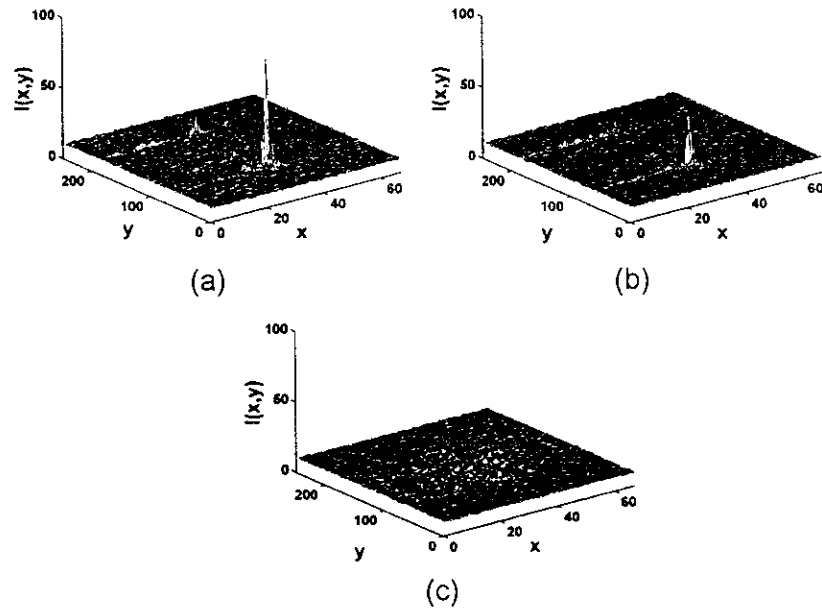
4.2.2 Multiple-Target Detections

Figure 4.3 Experimental results of the multiple-fingerprint detection. (a) Correlation output by using the uncompressed fingerprint reference. (b-c) correlation outputs by using the compressed reference (QF = 10) under a situation that the target is: (b) noise free and (c) noisy ($\sigma^2 = 1$).

Figures 4.3(a), (b), and (c) show the experimental outputs obtained from the detections of the multiple-fingerprint. The correlation output shown in Fig. 4.3(a) consists of two distinctive peaks with different heights. The peak with higher height corresponds to the autocorrelation of the uncompressed high-contrast fingerprint, while the low peak is generated by the cross correlation of the reference and the non-target fingerprint. The correlation peaks obtained from the detection of the target and of the non target are referred as the primary and the secondary peaks, respectively. The decrease of both correlation peaks caused by the detection of the noise-free multiple-fingerprint by the compressed reference with QF = 10 can be seen from Fig. 4.3(b). Figure 4.3(c) shows the detection of the noisy multiple-fingerprint target with variance $\sigma^2 = 1$ by using the reference compressed at QF = 10. It shows that no apparent correlation peaks are detected. In particular, the secondary correlation peak is minimized.

Figure 4.4(a) shows the 3-D plot of the correlation outputs of the multiple-face detection using the uncompressed human face reference, while Figs. 4.4(b) and (c) illustrate the correlation outputs using the compressed reference with QF = 10. It can be seen from Fig.

4.4(a) that the primary correlation peak intensity is higher and sharper than that of the secondary peak. When the reference is compressed, the degradation of the primary peak intensity shown in Fig. 4.4(b) is insignificant compared to the secondary peak. However, when the multiple-target is strongly corrupted by the noise, there are no observable correlation peaks that can be seen from Fig. 4.4(c).
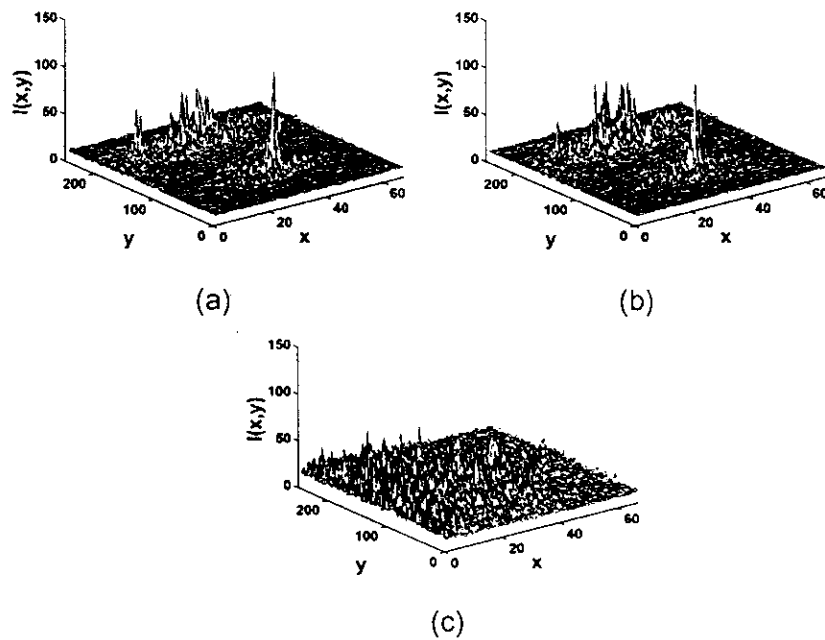

Figure 4.4 Experimental results of the multiple-human-face detection. (a) Correlation output by using the uncompressed human face reference. (b-c) correlation outputs by using the compressed reference (QF = 10) under a situation that the target is: (b) noise free and (c) noisy ($\sigma^2=1$).

Chapter 5

Conclusions

Real-time implementation of the JTC by using the JPEG-compressed reference images has been studied and experimentally demonstrated. The experimental results confirm the feasibility of implementing the JTC with compressed reference images. However, unlike the simulation results, the effect of the additive noise on the detection performance of the proposed JTC is more severe than that of the compression. This may be caused by the speckle noise which is inherently generated as a result of light scattering and multiple internal reflections that come from the EASLM and the CCD sensor. This study reveals that the storage problem and the time response acceleration of the non-destructive testing can be solved by using the JTC with compressed reference images.

References

1. R.K. Erf, *Holographic Non-destructive Testing*, Academic Press, New York, 1974.

2. R. Bexon, M.G. Dalzell, and M.C. Stainer, "In-line holography and the assessment of aerosols," Opt. Laser Tech. **8**, pp. 161-165 (1976).

3. G.A. Tyler and B.J. Thompson, "Fraunhofer holography applied to particle size analysis: a reassessment," Opt. Acta **23**, pp. 685-700 (1976).

4. P.R. Payne, K.L. Carder, and R.G. Steward, "Image analysis for holograms of dynamic oceanic particles," Appl. Opt. **23**, pp. 204-210 (1984).

5. H.J. Vossing, S. Burrmann, and R. Jaenicke, "In-line holography of cloud volumes applied to measurement of raindrops and snowflake," Atmos. Res. **49**, pp. 199-212 (1998).

6. J. Widjaja, "Automatic holographic particle sizing using wavelet-based joint transform correlator," Optik **107**, pp. 132-134 (1998).

7. W. B. Pennebaker and J.L. Mitchell, *JPEG Still Image Data Compression Standard*, New York: Van Nostrand Reinhold, 1993.

8. Http://homepages.borland.com/jedi/jcl/

9. Http://www.hicomponents.com/nindex.asp.

10. J. Widjaja and U. Suripon, "Real-time joint transform correlator by using compressed reference images," in *Special Issue: Trends in Pattern Recognition, Algorithms, and Devices*. Opt. Eng. **43**, pp. 1737-1745 (2004).

11. J. Widjaja and U. Suripon, "Multiple-target detection by using joint transform correlator with compressed reference images," Opt. Commun. **253**, pp. 44-55 (2005).

12. J. Widjaja and U. Suripon, "Experimental verifications of joint transform correlator using compressed reference images," Appl. Opt. **45**, pp. 8074-8082 (2006).

Curriculum Vitae

1. Name: Joewono WIDJAJA

2. Current position: Associate Professor

3. Educational background:
> 1986 Bachelor of Engineering (Electronic), Satya Wacana Christian Univ., Indonesia
> 1991 Master of Engineering (Electronic), Hokkaido University, Japan
> 1994 Doctor of Engineering (Electronic), Hokkaido University, Japan

4. Field of specialization: Optical information processing

5. List of publications:

1. J. Widjaja and Y. Tomita, "Optical wavelet-matched filtering by four-wave mixing in photorefractive media," Opt. Commun. **117**, pp. 123-126 (1995).
2. J. Widjaja and Y. Tomita,"Optical triple-in digital logics using non-linear optical four-wave mixing," Appl. Opt. **34**, No. 23, pp. 5074-5076 (1995).
3. J. Widjaja, Y. Tomita, and A. Wahab, "Application of wavelet-matched filters to holographic associative memories," Opt. Commun. **132**, 217-220 (1996).
4. J. Widjaja and Y. Tomita, "Particle-image velocimetry using wavelet-matched filters," J. Mod. Opt. **43**, 1993-1997 (1996).
5. J. Widjaja, "Spatial-angular multiplexed 3-d holographic memory using zone plates and 1-d grating," Opt. Mem. Neural Net. **6**, pp. 125-127 (1997).
6. J. Widjaja, "Automatic holographic particle sizing using wavelet-based joint transform correlator", Optik **107**, pp. 132-134(1998).
7. J. Widjaja, J. Uozumi, and T. Asakura, "Real-time specklegram analysis using wavelet-matched filters, " Asian J. Phys. **7**, No. 1, pp. 37-41 (1998).
8. J. Widjaja and S. Jutamulia, "Use of wavelet analysis for improving autofocusing capability," Opt. Commun. **151**, pp. 12-14 (1998).
9. J. Widjaja, "Dynamic optical processing of 2-D wavelet transforms," Opt. Mem. Neural Net. **8**, pp. 75-79 (1999).
10. J. Widjaja, "Wavelet transform for autofocusing detection systems," Sci. Asia **26**, pp. 111-114, (2000).
11. J. Widjaja, N. Wada, Y. Ishii, and W. Chujo, "Photonic packet address processor using holographic correlator," Elect. Lett. **37**, pp. 703-704 (2001).
12. J. Widjaja, "IP router using optical address recognition with second-harmonic generator," Elect. Lett. **38**, pp. 1268-1270 (2002).
13. S. Soontaranon, J. Widjaja, and T. Asakura, "Direct analysis of in-line particle holograms by using wavelet transform and envelope reconstruction method," Optik **114**, pp. 489-494(2002).
14. J. Widjaja, "Effects of image compression on digital specklegrams," in *Special Issue: Trends in Digital Speckle Pattern Interferometry*, Opt. Lasers Eng. **39**, pp. 501-506 (2003).
15. J. Widjaja, "Spectral-hologram-based correlator for photonic IP router: Architectural Considerations," Opt. Eng. **42**, pp. 747-752 (2003).
16. J. Widjaja, 'Wavelet transform correlator," in Encyclopedia of Optical Engineering, R.G. Driggers, Ed., pp. 2993 - 2999, Marcel Dekker, New York (2003).

17. J. Widjaja and U. Suripon, "Real-time joint transform correlator by using compressed reference images," in *Special Issue: Trends in Pattern Recognition, Algorithms, and Devices.* Opt. Eng. **43**, pp. 1737-1745 (2004).

18. H. Hui, F.J. Song, J. Widjaja, and J.H. Li, "ANFIS-based fingerprint-matching algorithm," in *Special Issue: Trends in Pattern Recognition, Algorithms, and Devices.* Opt. Eng. **43**, pp. 1814-1819 (2004).

19. S. Soontaranon, J. Widjaja, and T. Asakura, "Improved holographic particle sizing by using absolute values of the wavelet transform," Opt. Commun **240**, pp. 253-260 (2004).

20. J. Widjaja, "Particle sizing by using wavelet transform of compressed digital in-line holograms," Opt. Mem. Neural Net. **13**, pp. 189-194 (2004).

21. J. Widjaja and U. Suripon, "Multiple-target detection by using joint transform correlator with compressed reference images," Opt. Commun. **253**, pp. 44-55 (2005).

22. J. Widjaja, "Objective evaluation of information retrieved from digitally-compressed in-line holograms," Opt. Lasers Eng. **44**, pp. 1239-1251 (2006).

23. J. Widjaja and U. Suripon, "Experimental verifications of joint transform correlator using compressed reference images," Appl. Opt. **45**, pp. 8074-8082 (2006).